International Journal of Materials Science
ISSN 0973-4589 Volume 5, Number 3 (2010), pp. 393-397

https://dx.doi.org/10.37622/IJoMS/5.3.2010.393-397

Effect of Structural Morphology on the Electrochemical Behaviour of $Ni_{78}Si_8B_{14}$ alloy in 1 M HNO_3 Aqueous Medium

Shubhra Mathur*, Rishi Vyas, K. Sachdev and S.K. Sharma

Department of Physics, Malaviya National Institute of Technology, Jaipur- 302017, India

Abstract

The electrochemical behaviour of air side and wheel side surfaces of the melt-spun ribbon $Ni_{78}Si_8B_{14}$ was investigated using potentiodynamic polarization method in 1 M HNO_3 aqueous medium at room temperature. It was observed that the corrosion current density on the air side surface was less as compared to the wheel side surface of the specimen of the alloy $Ni_{78}Si_8B_{14}$. The observed behaviour can be related to the surface morphology due to processing of the ribbons. Weight loss studies carried out on these specimens corroborates the polarization results.

Keywords: Amorphous, Alloy, Corrosion, XRD.

Introduction

Metallic glasses (amorphous alloys) are known to have good mechanical properties, high corrosion resistance and a high hydrogen-adsorption property. They require a high cooling rate of 10^5-10^6 K/s and the bulk amorphous alloys require a cooling rate of 1-100 K/s for formation [1]. Metallic glasses exhibit superior corrosion resistance as compared to their crystalline counterparts because of the absence of defects such as grain boundaries, vacancies and dislocations [2-4].

Thus it is important to know the difference in the electrochemical behaviour when both the air side surface and wheel side surface exhibits amorphous nature. This motivated us to compare the corrosion behaviour of the air side surface and the wheel side surface of the melt spun ribbon $Ni_{78}Si_8B_{14}$ in 1 M HNO_3 aqueous medium at room temperature.

Experimental

The amorphous nature of the air side and wheel side surfaces of the melt–spun ribbon $Ni_{78}Si_8B_{14}$ was confirmed by X-ray diffraction (XRD). The X-ray diffraction pattern was recorded using CuK_α radiation at room temperature. The specimens of suitable size (1 cm x 1 cm x 30 μm) were cut from the melt-spun ribbon $Ni_{78}Si_8B_{14}$ in order to perform potentiodynamic polarization studies. The specimens were cleaned ultrasonically with ethanol and dried in air prior to inserting them in the corrosion cell for electrochemical studies. The potentiodynamic polarization studies were carried out on air side surface and wheel side surface of the alloy $Ni_{78}Si_8B_{14}$ using Echochemi (Model Autolab 30) in 1 M HNO_3 aqueous medium under identical experimental conditions. The experimental details and procedure for calculating the corrosion current density from polarization plots can be found in another paper [5]. Weight loss method was also employed in order to confirm the polarization data. The specimens of air side surface and wheel side surface of the amorphous alloy $Ni_{78}Si_8B_{14}$ were immersed for about 720 hours in 1 M HNO_3 aqueous medium. The corrosion rate is determined from the measured weight loss data using formula [6]:

Corrosion rate (mm/year) = 87.6 W/DAT

where T= time of exposure in hours, A = area of test specimen in cm^2, W = weight loss in (mg) and D = density of the test specimen in g/cm^3

Results

The X-ray diffraction (XRD) pattern of the air side surface and wheel side surface of the ribbon $Ni_{78}Si_8B_{14}$ is shown in Fig. 1. The X-ray diffraction pattern depicts that both air side surface and wheel side surface of the ribbon are amorphous in nature. Fig. 2 shows the potentiodynamic polarization plots of the air side and wheel side surface of the amorphous alloy $Ni_{78}Si_8B_{14}$ in 1 M HNO_3 aqueous medium. The corresponding values of corrosion current density are given in Table 1. It is observed that air side surface is more corrosion resistant as compared to wheel side surface of the specimen $Ni_{78}Si_8B_{14}$. Weight loss studies were also carried out in order to confirm the polarization results. The values of corrosion rate calculated from the weight loss data are mentioned in Table 1.

Fig. 3 shows the optical micrographs of air side surface and wheel side surface of the amorphous alloy after corrosion test in 1 M HNO_3 aqueous medium. It is observed that wheel side surface exhibits more corrosion as compared to the air side surface of the amorphous alloy $Ni_{78}Si_8B_{14}$.

Table 1: Potentiodynamic polarization results and weight loss data of the specimen $Ni_{78}Si_8B_{14}$ in 1 M HNO_3 aqueous medium at room temperature.

Alloy	**Polarization Results**	**Weight Loss Data**
$Ni_{78}Si_8B_{14}$	I_{corr} (A/cm^2)	Corrosion Rate (mm/year)
Air side surface	1.6×10^{-6}	2.1×10^{-2}
Wheel side surface	2.3×10^{-5}	5.2×10^{-2}

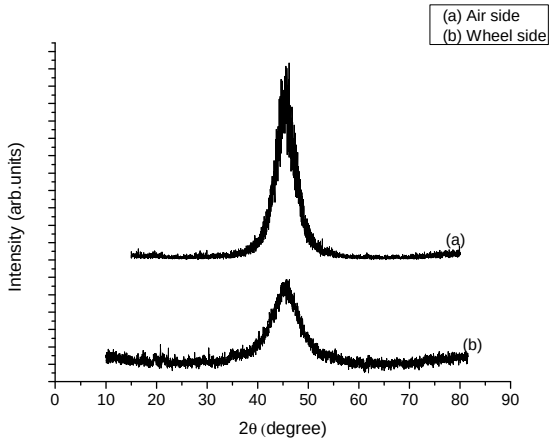

Figure 1: The X-ray diffraction pattern (XRD) of the specimen $Ni_{78}Si_8B_{14}$ for (a) air side surface (b) wheel side surface.

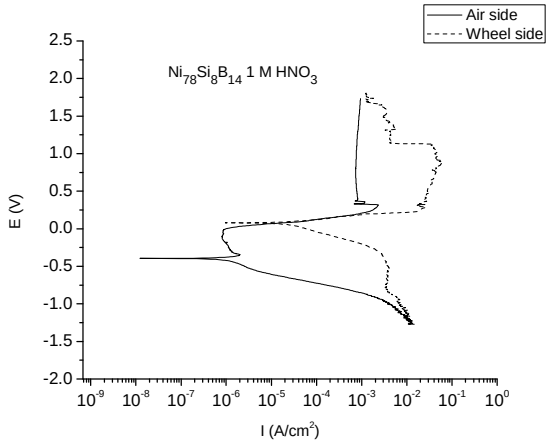

Figure 2: Potentiodynamic polarization plots for air side surface and wheel side surface of the amorphous alloy $Ni_{78}Si_8B_{14}$ in 1 M HNO_3 aqueous medium.

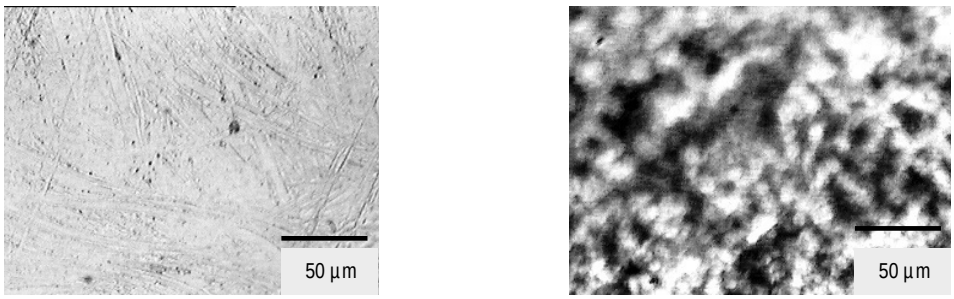

(a) (b)

Figure 3: Optical micrographs for the (a) air side and (b) wheel side of the melt spun ribbon $Ni_{78}Si_8B_{14}$ after corrosion test in 1 M HNO_3 aqueous medium.

Discussion

The high corrosion resistance of air side surface as compared to the wheel side surface of the amorphous alloy $Ni_{78}Si_8B_{14}$ can be understood in the light of the fact that the alloy was obtained by melt-spinning technique. During melt spinning, in the case of air side surface the air ejects to the outside. However in the case of wheel side surface, air entraps between wheel and ribbon surface due to the high speed of the wheel. This results in higher concentration of air pockets on the wheel side surface. The presence of these air pockets on the wheel side surface makes it appears as duller as compared to the air side surface. Further the higher cooling rate of the wheel side leads to higher concentration of quenched in defects. Hence the wheel side surface of the ribbon $Ni_{78}Si_8B_{14}$ in the present investigation shows inferior corrosion resistance as compared to the air side surface. It is noteworthy here that the results of the present investigations are also corroborated by weight loss studies and optical micrographs.

Similar investigations are reported by some investigators [7-8]. Dutta et al. reported that the wheel side surface of the Ti-Cu ribbon possess inferior corrosion resistance as compared to the air side surface. It was suggested that the higher concentration of air pockets favoured easier passive film breakdown by acting as pitting sites. In another investigation Vishwanadh et al. reported that the corrosion at the wheel side surface of the as cast melt-spun ribbon $Fe_{67}Co_{18}Si_{14}B_1$ was higher than the air side surface and it has been related to the surface morphology due to processing in the ribbons. Thus in the present investigation the air side surface of the ribbon $Ni_{78}Si_8B_{14}$ is more corrosion resistant as compared to the wheel side surface of the same alloy in 1 M HNO_3 aqueous medium.

Conclusions

1. Potentiodynamic polarization results revealed that the air side surface exhibits superior corrosion resistance as compared to the wheel side surface of the melt spun ribbon $Ni_{78}Si_8B_{14}$.
2. Weight loss studies also confirm the polarization results in 1 M HNO_3 aqueous medium at room temperature.

Acknowledgement

Thanks are due to Dr. M. –P. Macht, Hahn-Meitner-Institue, Berlin for supplying the melt spun ribbon $Ni_{78}Si_8B_{14}$.

References

[1] Klement, W., Willens, R. H., and Duwez, P., 1960, “Non-crystalline Structure in Solidified Gold-Silicon Alloys”, Nature, 187, pp. 869-870.

[2] Waseda, Y. and Aust, K. T., 1981, “Corrosion behaviour of Metallic Glasses”, J. Mater. Sci., 16, pp. 2337-2359.

[3] Scully, John R., Gebert, A., and Payer, Joe H., 2007, "Corrosion and Related Mechanical Properties of Bulk Metallic Glasses", J. Mater. Res., 22, pp. 302-313. .

[4] Mathur, Shubhra, Vyas, Rishi, Dolia, S. N., Sachdev, K., and Sharma, S. K., 2009, "Corrosion Behaviour of Amorphous and Nanocrystalline $Ti_{60}Ni_{40}$ in Aqueous HNO_3 Solution", Advanced Materials Research, 67, pp. 173-178.

[5] Dhawan, A., Sachdev, K., Roychowdhury, S., De, P. K., and Sharma, S. K., 2007, "Potentiodynamic Polarization Studies on Amorphous $Zr_{46.75}Ti_{8.25}Cu_{7.5}Ni_{10}Be_{27.5}$, $Zr_{67}Cu_{17.5}Ni_{10}Al_{7.5}$, $Zr_{67}Ni_{33}$ and $Ti_{60}Ni_{40}$ in Aqueous HNO_3 Solutions", J. Non-Cryst. Solids, 353, pp. 2619-2623.

[6] Fontana, Mars G., 1967,"Corrosion Engineering", McGraw-Hill International, III edition, Singapore, pp. 171-173.

[7] Dutta, R. S., and Dey, G. K., 2003, "Effect of Partial Crystallinity and Quenched in Defects on Corrosion of a Rapidly Solidified Ti-Cu Alloy", Bull. Mater. Sci., 26, pp. 477-482.

[8] Vishwanadh, B., Balasubramaniam, R., Srivastava D., and Dey, G. K., 2008, "Effect of Surface Morphology on Atmospheric Corrosion Behaviour of Fe-based Metallic Glass, $Fe_{67}Co_{18}Si_{14}B_1$", Bull. Mater. Sci., 31, pp. 693-698.